Stem Cell Reports
Article

ISSCR

OPEN ACCESS

Modeling the Pathogenesis of Charcot-Marie-Tooth Disease Type 1A Using Patient-Specific iPSCs

Lei Shi,[1,2,6] Lihua Huang,[3,6] Ruojie He,[1,6] Weijun Huang,[3] Huiyan Wang,[3] Xingqiang Lai,[3] Zhengwei Zou,[3] Jiaqi Sun,[3] Qiong Ke,[3] Minying Zheng,[1] Xilin Lu,[1] Zhong Pei,[1] Huanxing Su,[4] Andy Peng Xiang,[3,5] Weiqiang Li,[3,5,7,*] and Xiaoli Yao[1,*]

[1]Department of Neurology, National Key Clinical Department and Key Discipline of Neurology, Guangdong Key Laboratory for Diagnosis and Treatment of Major Neurological Diseases, The First Affiliated Hospital, Sun Yat-Sen University, Guangzhou 510080, China
[2]Division of Neurosurgical Intensive Care Unit, Department of Critical Care Medicine, The First Affiliated Hospital, Sun Yat-Sen University, Guangzhou 510080, China
[3]Center for Stem Cell Biology and Tissue Engineering, Key Laboratory for Stem Cells and Tissue Engineering, Ministry of Education, Sun Yat-Sen University, Guangzhou 510080, China
[4]State Key Laboratory of Quality Research in Chinese Medicine, Institute of Chinese Medical Sciences, University of Macau, Macao 999078, China
[5]Department of Biochemistry, Zhongshan Medical School, Sun Yat-sen University, Guangzhou 510080, China
[6]Co-first author
[7]Lead Contact
*Correspondence: liweiq6@mail.sysu.edu.cn (W.L.), liliyao71@163.com (X.Y.)
https://doi.org/10.1016/j.stemcr.2017.11.013

SUMMARY

Charcot-Marie-Tooth disease type 1A (CMT1A), one of the most frequent inherited peripheral neuropathies, is associated with *PMP22* gene duplication. Previous studies of CMT1A mainly relied on rodent models, and it is not yet clear how *PMP22* overexpression leads to the phenotype in patients. Here, we generated the human induced pluripotent stem cell (hiPSC) lines from two CMT1A patients as an *in vitro* cell model. We found that, unlike the normal control cells, CMT1A hiPSCs rarely generated Schwann cells through neural crest stem cells (NCSCs). Instead, CMT1A NCSCs produced numerous endoneurial fibroblast-like cells in the Schwann cell differentiation system, and similar results were obtained in a PMP22-overexpressing iPSC model. Therefore, despite the demyelination-remyelination and/or dysmyelination theory for CMT1A pathogenesis, developmental disabilities of Schwann cells may be considered as an underlying cause of CMT1A. Our results may have important implications for the uncovering of the underlying mechanism and the development of a promising therapeutic strategy for CMT1A neuropathy.

INTRODUCTION

Charcot-Marie-Tooth (CMT) disease, also known as hereditary motor and sensory neuropathies, was initially characterized in the late 19th century. It is the most frequent inherited neuropathy affecting the peripheral nervous system and is found in about 1 in 2,500 people. CMT constitutes a group of genetically and clinically heterogeneous disorders with similar clinical manifestations, including progressive weakness and atrophy of the distal muscles. CMT type 1A (CMT1A), the most common form of CMT, is associated with a 1.5-Mbp DNA duplication in the chromosome 17p11.2 region, which contains the *PMP22* gene (Lupski et al., 1991). Clinically, the symptoms of CMT1A patients are similar to those of other subtypes. On nerve biopsies, CMT1A patients usually exhibit loss of the myelin sheath and the onion bulbs of Schwann cell lamellae (Hanemann et al., 1997). Therefore, many researchers believe that CMT1A is caused by a PMP22-overexpression-mediated dysfunction of the demyelination-remyelination process in Schwann cells (Sereda et al., 1996). However, a study in CMT1A children found that all subjects had sharply decreased nerve conduction velocities that were evident at a very young age, prior to the onset of discomfort, and that this alteration did not show any further worsening with age (Berciano et al., 2000). Similarly, a study in CMT1A mice found that the sciatic nerves remained largely unmyelinated in neonatal mice, which exhibited only a few small myelinated fibers, and that the situation did not improve with age. The authors proposed that dysmyelination could be a major cause of the disease (Robaglia-Schlupp et al., 2002). However, as we lack information on the pathophysiological processes that occur during the asymptomatic phase of the disease, the underlying molecular mechanisms that lead to the CMT1A phenotype remain largely unknown. It is also not yet known whether *PMP22* duplication affects Schwann cell development and/or myelin sheath formation.

In vitro disease modeling using patient-derived stem cells is expected to be of great value for studying the mechanisms of disease pathogenesis. Reprogramming human somatic cells to a pluripotent state allows researchers to generate human induced pluripotent stem cells (hiPSCs), which were first established by Takahashi and Yamanaka (2006). Since then, studies have shown that skin fibroblasts transfected with retroviruses expressing *Oct4*, *Sox2*, *Klf4*, and *c-Myc* could be reprogrammed into embryonic stem cell (ESC)-like cells. iPSCs share many characteristics with ESCs, and

have the ability to self-renew and differentiate into cells of all three germ layers. Thus, iPSC technology offers a powerful tool for developmental biology research, drug discovery, and *in vitro* modeling of human disease (Hargus et al., 2014).

In vertebrates, neural crest generates most cells of the peripheral nervous system (PNS) (including peripheral neurons, Schwann cells, and endoneurial fibroblasts) and several non-neural cell types, including the craniofacial skeleton, the thyroid gland, the thymus, the cardiac septa, smooth muscles, melanocytes, among others (Anderson, 2000). Some of the neural crest cells that can self-renew and give rise to a variety of cell types are referred to as neural crest stem cells (NCSCs). In recent years, various researchers have described the efficient derivation and isolation of NCSCs from human PSCs, and their further differentiation into various cell types, including peripheral neurons, Schwann cells, and mesenchymal-lineage cells (e.g., osteoblasts, adipocytes, and chondrocytes) (Lee et al., 2007). Thus, NCSCs have become an ideal model system to study the normal development of PNS, and to understand the pathogenesis and identify the cures for PNS-related disorders.

Here, we successfully established an iPSC technology-based *in vitro* human model of CMT1A. Subsequently, to simulate developmental progress with the aim of studying probable pathogenic mechanisms and identifying potential therapies for CMT1A, we induced CMT1A-iPSCs to differentiate into Schwann cells via the NCSC stage. Interestingly, we found that the development of Schwann cells was interrupted and the generation of endoneurial fibroblasts was enhanced when CMT1A NCSCs (harboring the *PMP22* duplication) were cultured in the Schwann cell differentiation system.

RESULTS

CMT1A hiPSCs Exhibit the Characteristics of Self-Renewal and Pluripotency

Solochrome cyanine staining of peroneal nerve biopsies from patient 1 (CMT1A-1, with less severe symptoms) showed a lack of obvious onion bulbs and greatly reduced myelin formation (Figure 1A, middle panel) compared with normal samples (Figure 1A, left panel). In the sample from patient 2 (CMT1A-2, with more severe clinical manifestations), however, there was an almost total lack of myelin; instead, fibroblast-like cells filled the space (Figure 1A, right panel). These results confirmed the PNS neuropathy of these patients.

Skin tissue was subjected to adhesion culture for 7 days, and the obtained dermal fibroblasts (CMT1A hDFs) were easily propagated in high-glucose DMEM containing 10% fetal bovine serum (FBS) (data not shown). The extra copy of the PMP22 gene was verified using multiplex ligation-dependent probe amplification (MLPA) (Figure 1B) and no mutations were detected in the exons of all three copies of *PMP22* as revealed by Sanger sequencing (data not shown). The CMT1A hDFs were then exposed to culture supernatant containing retroviral vectors expressing four factors (*OCT4*, *SOX2*, *c-MYC*, and *KLF4*) or *GFP* (control) for 24 hr. The transfection efficiency was more than 90%, as illustrated by direct observation of GFP expression under a fluorescence microscope (data not shown). ESC-like colonies first emerged 10 days later; the cells had a high nucleus-to-cytoplasm ratio and prominent nucleoli. The iPSC generation efficiency was comparable between CMT hDFs and control hDFs (data not shown). Six colonies in total (three from each CMT1A hiPSC line, designated as CMT1A-1 hiPSCs and CMT1A-2 hiPSCs) were selected and expanded into stable cell lines and were used for further analyses. The CMT1A hiPSCs maintained their ESC-like morphology in long-term *in vitro* culture (data not shown). Immunocytochemistry showed that the control hiPSCs and CMT1A hiPSCs expressed the typical markers of pluripotent stem cells, including OCT4, SSEA4, and TRA-1-60 (Figure S1A). When spontaneous differentiation was induced *in vitro*, the control hiPSCs and CMT1A hiPSCs formed embryoid bodies (EBs). These EBs were then transferred to adherent culture on gelatin-coated plates, whereby the differentiated cells displayed various morphologies were positive for the endodermal marker α-fetoprotein, the mesodermal marker α-smooth muscle actin (αSMA), or the ectodermal marker tubulin β3 class III (TUBB3), as appropriate (Figure S1B). When the control hiPSCs and CMT1A hiPSCs were injected into SCID mice, teratomas were allowed to form for 2 months. Histological examination showed that the teratomas contained cells of all three germ layers, namely ectoderm-derived neural tubes, mesoderm-derived cartilage, and endoderm-derived glandular epithelium (Figure S1C).

NCSCs Can Be Efficiently Derived from CMT1A hiPSCs

Previous research showed that human ESCs and iPSCs can generate central and PNS components from neural precursors via an intermediate rosette stage (Lee et al., 2010). Here, we cultured CMT1A hiPSCs under conditions designed to generate NCSCs via EB formation, as previously described (Li et al., 2015). When EBs were adherently cultured in neural crest induction medium, neural rosettes emerged after 3 days of culture (Figure 2A). Numerous cells migrated out of the rosettes and were confirmed to express NCSC markers, such as SOX10, AP2α, P75, HNK1, and NESTIN (Figure 2B). When we used fluorescence-activated cell sorting (FACS) to purify NCSCs co-expressing p75 and HNK1, the differentiation efficiency of CMT1 hiPSCs (77.05% ± 2.94% in CMT1A-1 group; 81.51% ± 1.95% in

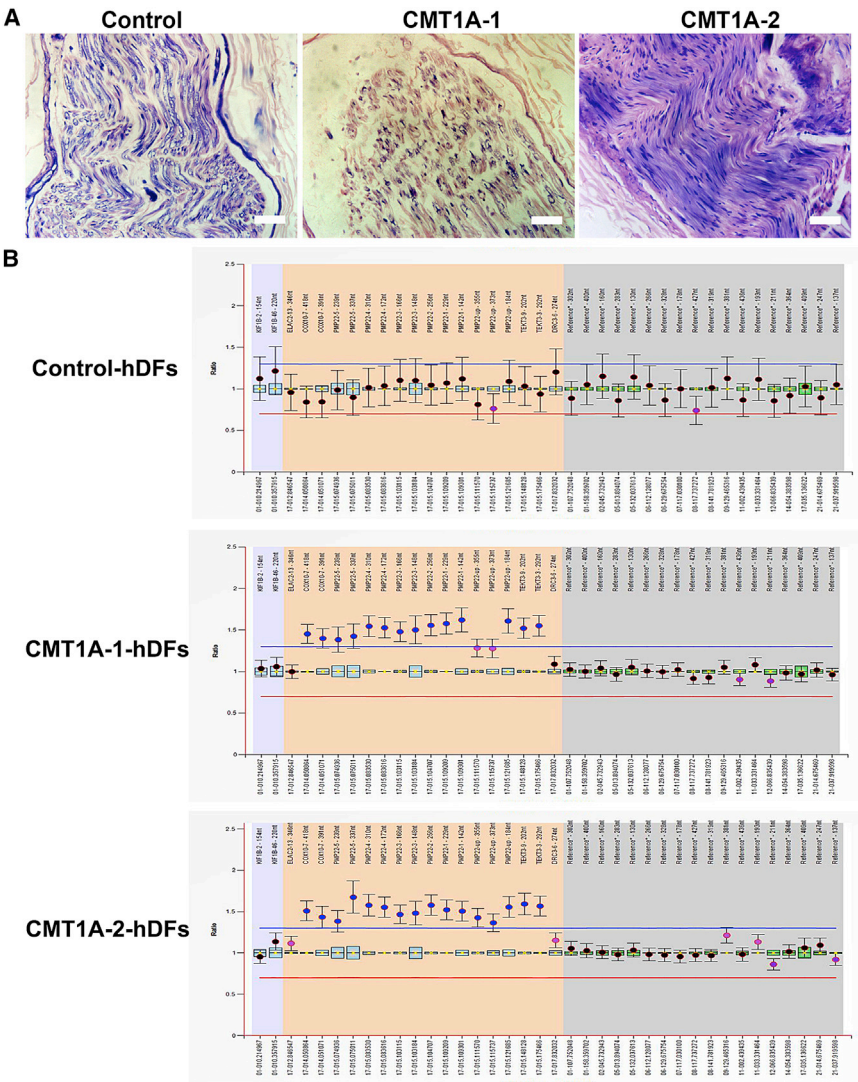

Figure 1. Solochrome Cyanine-Stained Nerve Biopsies of CMT1A Patients and MLPA Assay of CMT1A hDFs

(A) Solochrome cyanine staining of nerve biopsies from the CMT1A patient (middle for CMT1A-1 and right panel for CMT1A-2) was applied. The result showed that myelin formation is greatly reduced and numerous fibroblast-like cells exist in some areas in comparison with normal samples (left panel). Scale bars, 50 μm.

(B) MLPA assay (n = 3 independent experiments) was used for the diagnosis of CMT1A and confirmed that these two patients possessed the genomic *PMP22* duplication.

CMT1A-2 group) was not significantly different from that of control hiPSCs (78.68% ± 2.30%) after 8–10 days of differentiation ($p > 0.05$; Figure 3A; CMT1A-2, data not shown). The isolated CMT1A-1 NCSCs ($p75^+/HNK1^+$) were adherently cultured on poly-L-ornithine/laminin (PO/LN)-coated dishes (Figure 3B), and were confirmed to express the NCSC markers P75, HNK1, AP2α, SOX10, and SLUG (Figure 3C; CMT1A-2, data not shown). We also confirmed that CMT1A-1 NCSCs can be cultured in suspension, where they form spheres without losing the characteristic gene expression profile of NCSCs (data not shown).

CMT1A NCSCs Can Efficiently Differentiate to Mesenchymal Cell Lineages

Previous studies showed that NCSCs can be directed toward mesenchymal lineages, including osteogenic, adipogenic, and chondrogenic lineages, as well as smooth muscle cells (Lee et al., 2007). Here, we tested whether CMT1A NCSCs had a similar mesenchymal differentiation potential. We cultured CMT1A NCSCs in α-minimal essential medium containing 10% FBS. After 1 week, mesenchymal stem cells (MSCs) emerged and began proliferating rapidly (data not shown). FACS analyses showed that about 90% of CMT1A MSCs co-expressed the typical MSC surface markers, CD44 and CD73; in this, they were comparable with control cells (data not shown). To further assess the multi-lineage differentiation ability of CMT1A MSCs, we used various media to differentiate the cells into osteoblasts, adipocytes, chondrocytes, and smooth muscle cells. Alizarin red S staining, oil red O staining, toluidine blue staining, and anti-αSMA immunostaining confirmed that the CMT1A MSCs showed the capacity to differentiate into (respectively) osteogenic, adipogenic, and chondrogenic lineages, as well as smooth muscle cells (data not shown). The qRT-PCR results

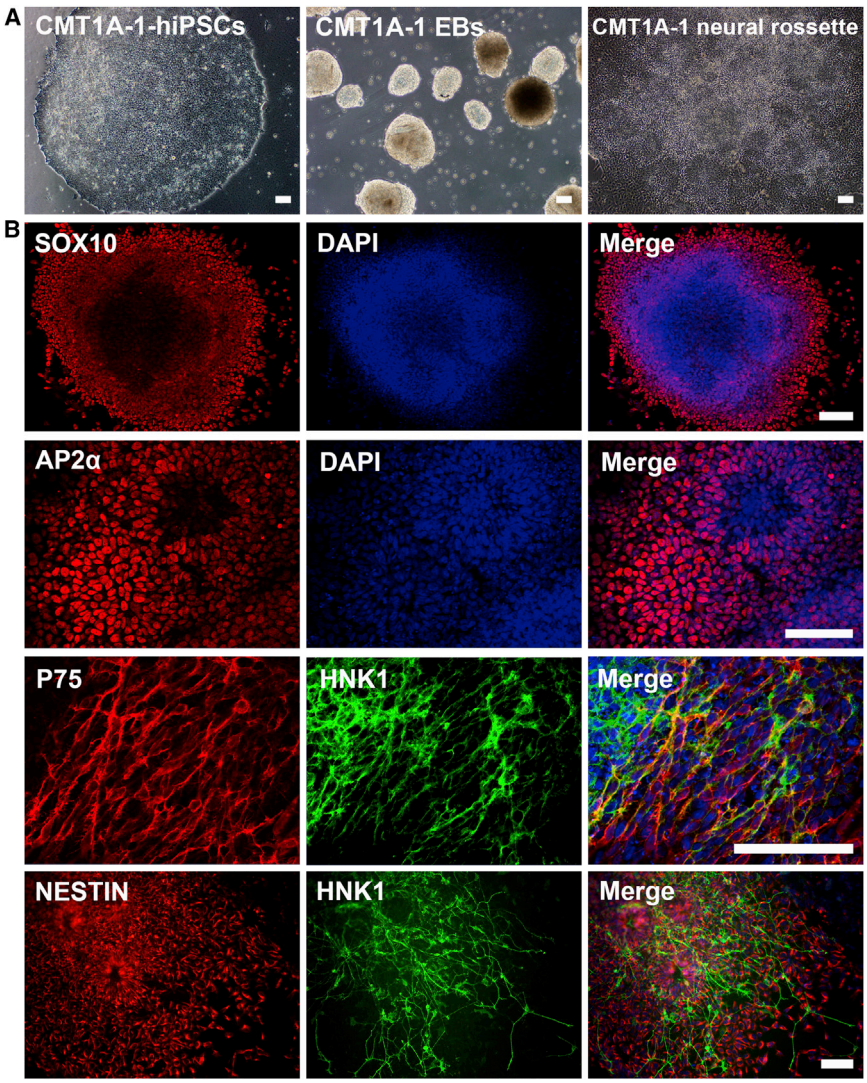

Figure 2. Neural Crest Differentiation of CMT1A hiPSCs

(A) Human iPSCs were cultured in E8 medium and plated on Matrigel-coated plates. The cells were cultured in neural crest induction medium for 5 days in ultra-low-attachment culture dishes, whereupon they clustered to form uniform EBs. The cells were then replated onto PO/LN-coated plates, and multiple rosette structures formed in the centers of the attached EBs (n = 5 independent experiments).

(B) Immunofluorescence analyses showed that cells migrating out from the rosette structures expressed the neural crest-specific markers SOX10, AP2α, P75, HNK1, and NESTIN.

Scale bars, 100 μm.

further confirmed the multi-lineage differentiation ability of CMT1A-1 MSCs (data not shown).

CMT1A NCSCs Possess the Potential to Differentiate into Peripheral Neurons

For peripheral neuronal differentiation, CMT1A NCSCs were cultured in a neuronal induction medium containing brain-derived neurotrophic factor, glial cell-derived neurotrophic factor, nerve growth factor, and dibutyryl cyclic AMP (db-cAMP). After 4–6 weeks, these cells exhibited a mature neuronal morphology (data not shown). Most of the differentiated cells expressed the pan neural marker, TUBB3 (86.75% ± 7.32% in the CMT1A-1 group, 80.37% ± 7.79% in the CMT1A-2 group, and 82.46% ± 6.63% in the control group), and the peripheral neuronal markers, PERIPHERIN (71.12% ± 5.91% and 75.88% ± 2.71%, respectively), BRN3A (46.21% ± 3.48% and 49.55% ± 5.09%, respectively), and tyrosine hydroxylase (18.03% ± 3.04% and 21.68% ± 4.27%, respectively) ($p > 0.05$; data not shown). The qPT-PCR analyses confirmed the expressions of these peripheral neuronal markers, and revealed that their levels were similar in the CMT1A and control groups (data not shown).

CMT1A NCSCs Display a Severe Defect in Schwann Cell Differentiation

For Schwann cell differentiation, CMT1A NCSCs were passaged for more than 2 months as described previously (Lee et al., 2010). These cells were then induced for 3 weeks in medium containing ciliary neurotrophic factor, neuregulin-1, and db-cAMP. Our serial observation under phase-contrast microscopy revealed significant differences

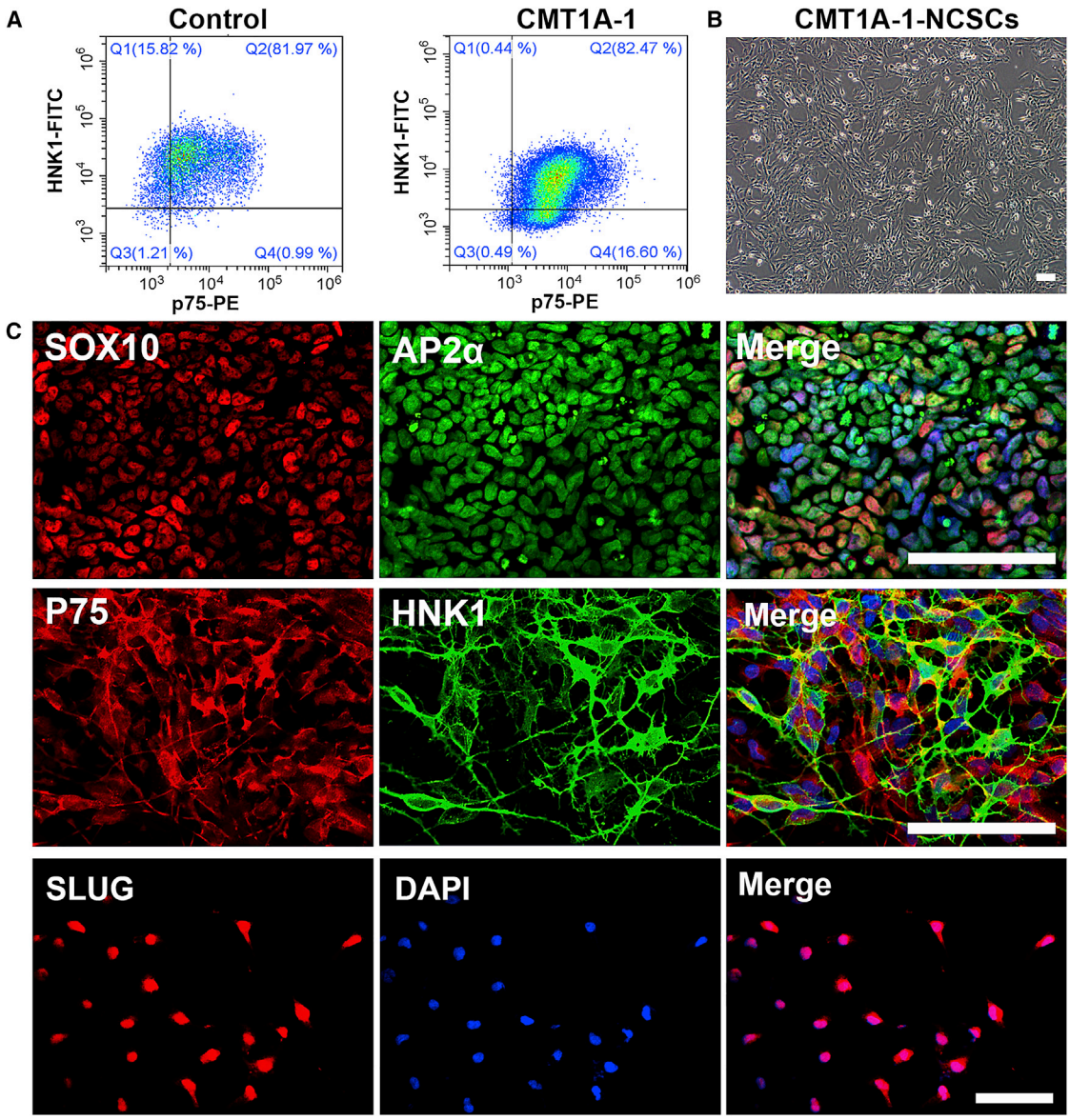

Figure 3. Enrichment and Characterization of CMT1A NCSCs

(A) hiPSCs were subjected to *in vitro* differentiation, and HNK1$^+$/P75$^+$ cells were isolated by FACS (n = 4 independent experiments).

(B) CMT1A NCSCs cultured on PO/LN-coated dishes maintained their typical cellular morphology.

(C) CMT1A NCSCs expressed the neural crest stem cell markers SOX10, AP2α, P75, HNK1, and SLUG.

Scale bars, 100 μm.

between CMT1A-1 and control cells. On day 5 after induction, almost all of the NCSCs in the control group showed morphological changes; some exhibited the typical bipolar spindle-shaped morphology of Schwann cells, while others were multipolar and star shaped. In the CMT1A-1 group, in contrast, only a small proportion of the NCSCs showed morphological changes, and very few were bipolar and spindle shaped. On day 10 post induction, the typical bipolar Schwann-like cells were more numerous in control cultures. Such cells were rarely seen in CMT1A-1 cultures, in which fibroblast-like cells emerged and proliferated quickly. On day 20, almost all of the cells in control group had become typical bipolar spindle-shaped cells, whereas CMT1A-1 cultures had become confluent with fibroblast-like cells (Figure 4A). Similar cellular morphological changes were also observed in CMT1A-2 cultures (data not shown). We used immunostaining to identify the differentiated cells. The Schwann cell markers, glial

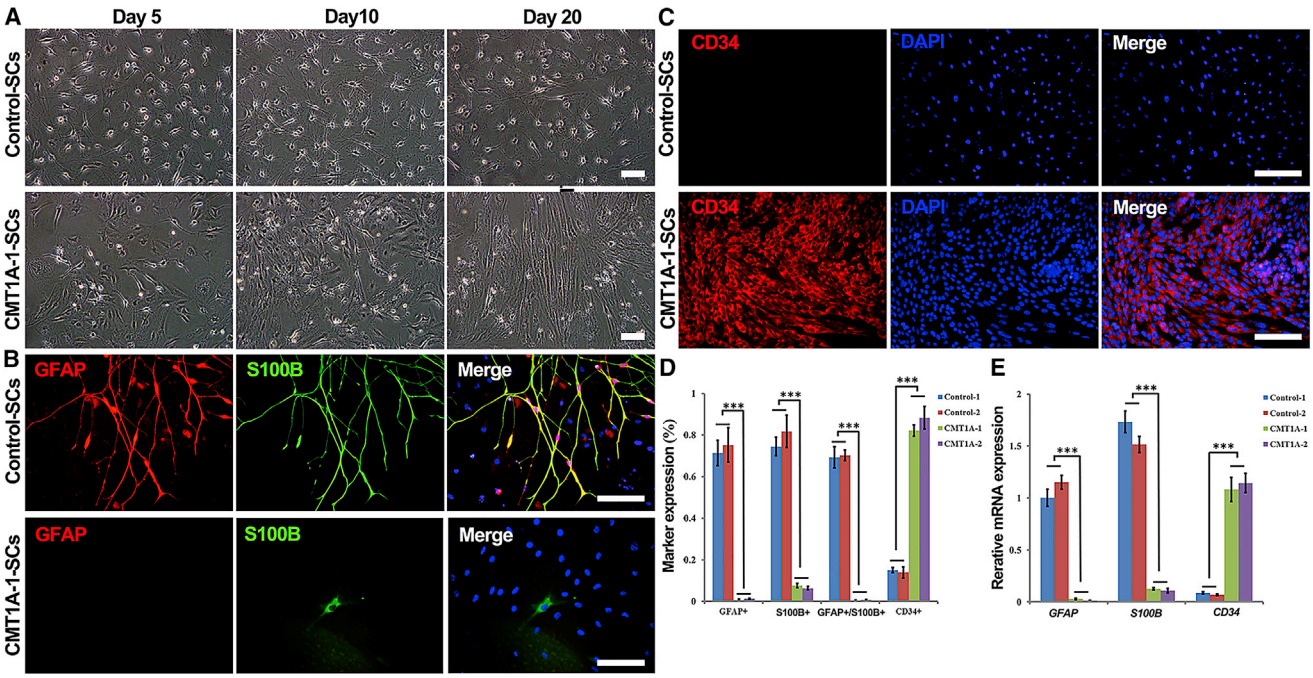

Figure 4. CMT1A NCSCs Were Induced to Differentiate into Schwann Cells

(A) Serial observation (days 5, 10, and 20) of Schwann cell differentiation under phase-contrast microscopy (n = 5 independent experiments) revealed that almost all control cells became typical bipolar and spindle-shaped cells, whereas those of the CMT1A group became confluent fibroblast-like cells.

(B) Immunostaining showed that differentiated cells in the control group strongly express the Schwann cell markers GFAP and S100B, whereas those in the CMT1A group do not.

(C) Differentiated cells in CNT1A group express the endoneurial fibroblast-specific marker, CD34, whereas few cells in the control group express this marker.

(D) The percentages of $GFAP^+$, $S100B^+$, and $CD34^+$ cells that differentiated from CMT1A and control NCSCs were compared (n = 5 independent experiments; ***$p < 0.001$).

(E) qRT-PCR analyses (n = 5 independent experiments) further confirmed that the mRNA expression levels of *GFAP/S100B* and *CD34* were higher and lower, respectively, in the control group versus the CMT1A group (***$p < 0.001$).

Scale bars, 100 μm.

fibrillary acidic protein (GFAP) and S100B, were strongly expressed in the control group (68.4% ± 4.39% and 74.0% ± 4.85% positive cells, respectively) but not the CMT1A group (0.11% ± 0.023% and 4.80% ± 0.84%, respectively). In contrast, CD34, which is a specific marker of endoneurial fibroblast-like cells (EFLCs) (Richard et al., 2012), was commonly expressed in the CMT1A group but not the control group (***$p < 0.001$; Figures 4B–4D). A previous study showed that NCSC-derived Schwann cell progenitors have the potential to generate endoneurial fibroblasts during the development of peripheral nerves via a process that is regulated by neuregulin, notch ligands, and bone morphogenic proteins (BMPs) (Joseph et al., 2004). qRT-PCR showed that the mRNA expression levels of *GFAP* and *S100B* were higher in the control group than in the CMT1A group, whereas CD34 showed the opposite pattern (***$p < 0.001$ for all comparisons; Figure 4E). These results suggest that CMT1A NCSCs generate few Schwann cells (those expressing GFAP and S100B) in the Schwann cell differentiation system, and instead differentiate to numerous $CD34^+$ EFLCs, indicating that increased *PMP22* gene dosage may cause the change of Schwann cell differentiation direction.

We also detected the expression of GFAP/S100B, myelin basic protein (MBP), and CD34 by immunofluorescence assay in peroneal nerve biopsy samples from controls and CMT1A patients. The results showed that intensively positive expression and significantly higher proportion of $GFAP^+/S100B^+$ and MBP^+ cells were detected in controls than that of CMT1A patients. Nonetheless, CD34 was weakly stained and fewer $CD34^+$ cells were found in control samples, although CD34 was strongly expressed in samples from the CMT1A group. Intriguingly, we also discovered that more $GFAP^+/S100B^+$ and MBP^+, cells and fewer $CD34^+$ cells existed in the nerve biopsy sample from CMT1A-1 (with less severe symptoms) than that from

CMT1A-2 (with more severe clinical manifestations) (Figures S2A and S2B). These results reflected that the *in vivo* development of Schwann cells in CMT1A patients might be interrupted by the duplication of *PMP22*, which was also consistent with the outcomes from the *in vitro* differentiation assay. Moreover, these results inferred that the expression level of GFAP/S100B and MBP in peripheral neural tissues was negatively correlated with the clinical severity, while the CD34 expression was positively correlated with the clinical severity.

Lentivirus-Mediated PMP22 Overexpression in Control hiPSCs Recapitulates the Defective Schwann Cell Differentiation of CMT1A hiPSCs

To further confirm this observation, we then examined whether *PMP22* overexpression in control hiPSCs impacted their ability to differentiate to Schwann cells. We transduced control hiPSCs with a PMP22-encoding lentivirus or the empty vector and used puromycin selection to isolate PMP22 hiPSCs and the transduction control. Immunofluorescence staining and western blotting confirmed that PMP22 was successfully overexpressed in PMP22 hiPSCs (data not shown). The western blot analysis also revealed that hiPSCs derived from controls and CMT1A patients expressed low levels of PMP22 protein when cells remained undifferentiated. Moreover, these cells retained the characteristics of iPSCs, including self-renewal and pluripotency, as illustrated by the expressions of OCT4, NANOG, and SSEA4, and the capacity to differentiate into three germ layer lineages *in vitro* and *in vivo* (data not shown).

We then evaluated the neural crest differentiation potential of PMP22 hiPSCs. FACS analyses showed that PMP22 hiPSCs, control hiPSCs, and CMT1A hiPSCs had similar abilities to generate $P75^+/HNK1^+$ NCSCs with high efficiency. The isolated PMP22 NCSCs can be adherently cultured on PO/LN-coated dishes. PMP22 NCSCs also expressed NCSC-specific markers (SOX10, P75, and HNK1; data not shown) and were similar to control hiPSCs and CMT1A hiPSCs in their ability to differentiate into mesodermal lineages and peripheral neurons (data not shown). However, when cultured under Schwann cell-differentiating conditions for 3 weeks, PMP22 NCSCs phenotypically resembled CMT1A-1 NCSCs and the cultures contained numerous fibroblast-like cells; similar cellular morphological change could also be observed in the Schwann cell differentiation process in CMT1A-2 NCSCs (data not shown); in this respect they were unlike the Schwann cell-differentiated control NCSCs, which were largely bipolar and spindle shaped (Figure 5A). The GFAP/S100B immunostaining of different colonies from control-1 hiPSCs, control-2 hiPSCs, CMT1A-1 hiPSCs, and CMT1A-2 hiPSCs are shown in Figure S3. FACS analyses showed that over 90% of the differentiated cells in the CMT1A and PMP22 groups expressed the endoneurial fibroblast-like cell marker, CD34, while only a small population of control cells was $CD34^+$ (Figures 5B and S4). The results of qRT-PCR (Figure 5C) and immunostaining assays (Figures 6, S3, and S4) also demonstrated that the increased *PMP22* gene dosage in the cells from CMT1A-1, CMT1A-2, and PMP22 groups was associated with a developmental switch in the Schwann cell differentiation of NCSCs toward EFLCs.

Previous study has demonstrated that PMP22 participates in cell proliferation and apoptosis (Li et al., 2013). To monitor the proliferation/apoptosis state of Schwann cell-differentiated cells in different groups, we performed anti-Ki67 immunostaining, whereby the results indicated that significantly more Ki67-positive cells could be found in CMT1A-1, CMT1A-2, and PMP22 groups than in the control group (Figures S5A and S5B). By contrast, no obvious cell apoptosis was detected by TUNEL assay at different time points during the Schwann cell differentiation process in all groups (data not shown). A previous report (Joseph et al., 2004) demonstrated that BMP4, NRG1, and DLL1 promote endoneurial fibroblast differentiation from NCSCs. We thus tried to determine whether the mRNA expression of *BMP4*, *NRG1*, and *DLL1* were highly upregulated in cells of the CMT1A group during Schwann cell differentiation. The results of qRT-PCR showed no significant difference in the expression level of all three genes between the control group and the CMT1A/PMP22 group at different differentiation stages (Figure S5C). The result indicated that the increase of endoneurial fibroblast differentiation potential of CMT1A NCSCs may be due to other intrinsic factors and need further investigation. It was reported that the decreased phosphatidylinositol 3-kinase (PI3K)-AKT activity and hyperactivation of the MEK-ERK pathway was observed in CMT rats (Fledrich et al., 2014). We thus used western blotting to monitor the protein level of AKT, pAKT, ERK, and pERK in Schwann cells from different groups. We found that, indeed, Schwann cells from CMT1A/PMP22 had higher ERK activation than controls. However, similar PI3K-AKT phosphorylation level was detected in control and CMT1A/PMP22 groups (Figure S5D). These results further implicated that the Schwann cell differentiation defect of CMT1A NCSCs may be partly due to elevated MEK-ERK activation. We also detected the PMP22 protein expression in NCSCs and Schwann cells from different groups. This result demonstrated that the PMP22 was expressed in cells of NCSC and Schwann cell stages from all groups. Meanwhile, cells from the CMT1A group expressed a higher level of PMP22 than that in control cells; however, no obvious difference was observed between CMT1A-1 and CMT1A-2 (Figure S5E).

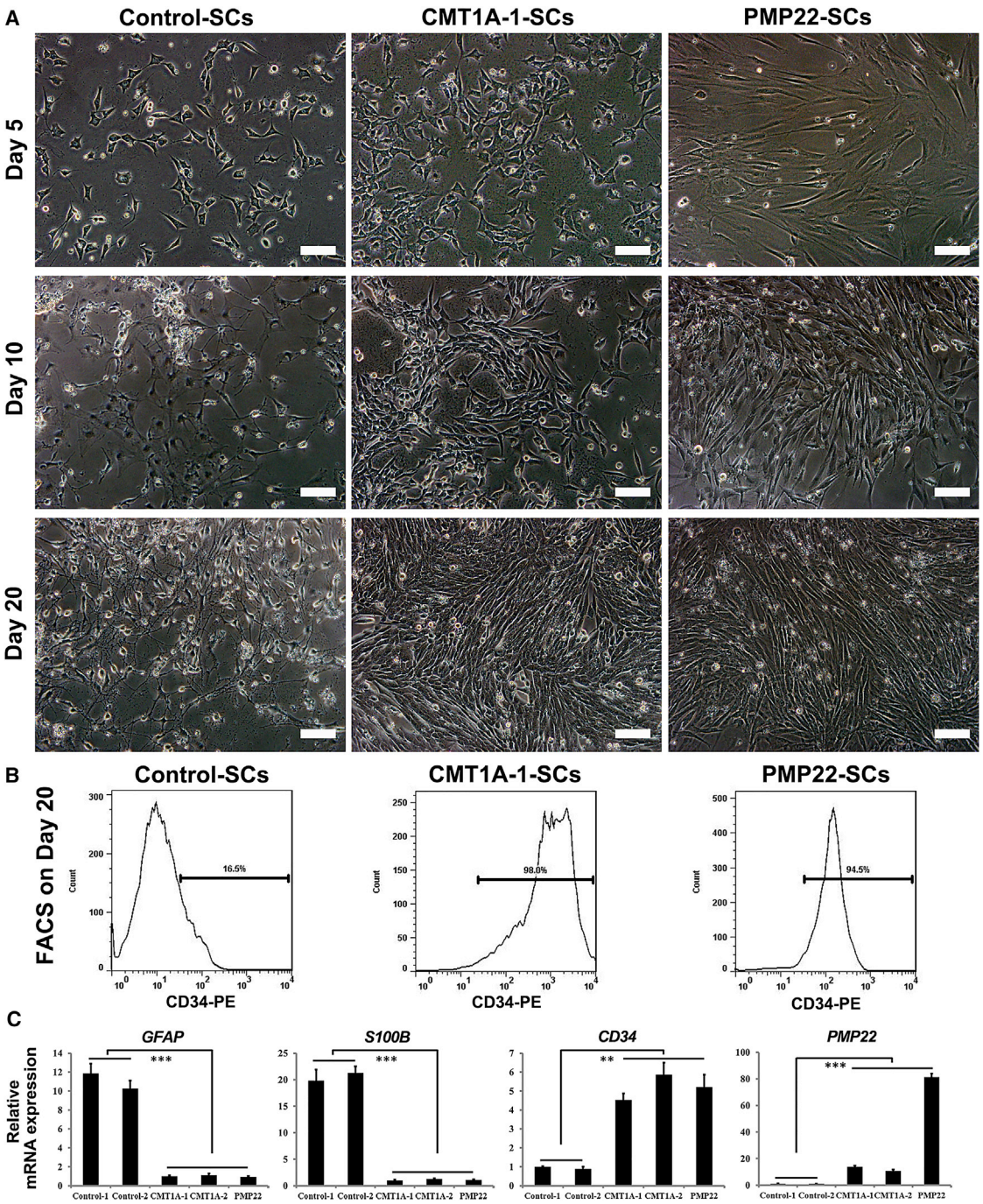

Figure 5. Schwann Cell Differentiation of PMP22 NCSCs

(A) Serial observation (days 5, 10, and 20) under phase-contrast microscopy (n = 4 independent experiments) revealed that most control cells became typical bipolar and spindle-shaped cells, while the cells of the CMT1A and PMP22 groups became confluent fibroblast-like cells. Scale bars, 100 μm.

(B) FACS analyses (n = 4 independent experiments) showed that over 90% of the differentiated cells in the CMT1A and PMP22 groups expressed CD34, while only a small population of control cells was $CD34^{+}$.

(C) qRT-PCR (n = 4 independent experiments) indicated that differentiated cells of the CMT1A and PMP22 groups had higher mRNA expression levels of *PMP22* and *CD34*, but lower mRNA expression levels of *GFAP* and *S100B*, compared with the control group (**p < 0.01, ***p < 0.001).

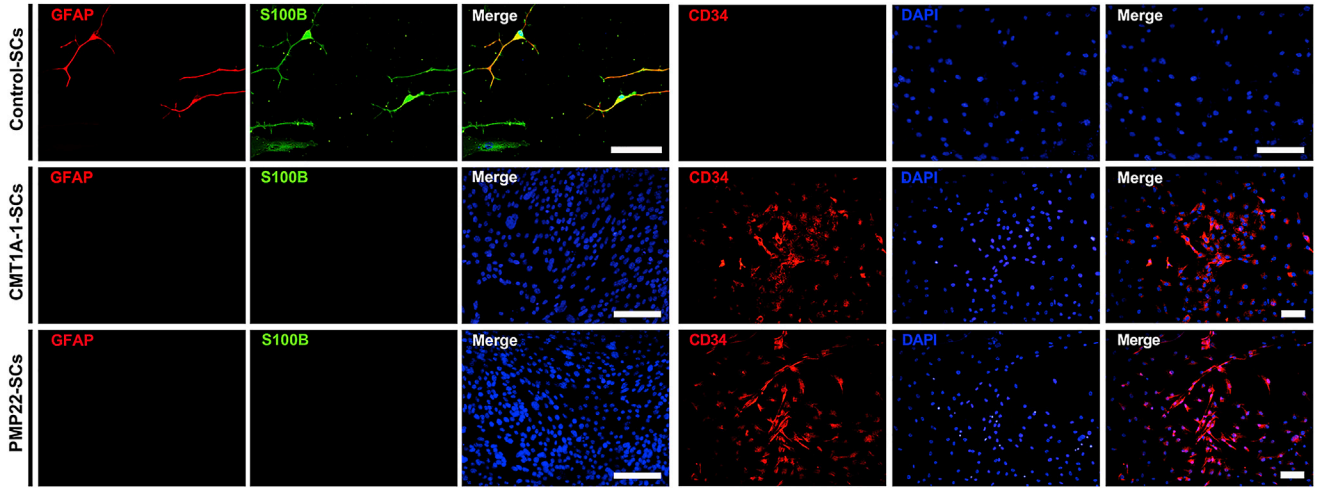

Figure 6. Immunostaining of NCSCs Subjected to Schwann Cell Differentiation

Differentiated control cells strongly expressed the Schwann cell markers, GFAP and S100B, but showed little expression of the endoneurial fibroblast marker, CD34. Conversely, cells of the CMT1A and PMP22 groups showed little expression of GFAP and S100B, but most of them were $CD34^+$ (n = 4 independent experiments). Scale bars, 100 μm.

More importantly, to determine whether Schwann cells derived from NCSCs have myelination ability, Schwann cells were added to the peripheral neurons differentiated from NCSCs originating from the same hiPSC and co-cultured for 3–4 weeks. Anti-MBP/PERIPHERIN staining showed that Schwann cells of the control group generated myelin segments and ensheathed bundles of axons, whereas Schwann cells from CMT1A-1, CMT1A-2, and PMP22 groups did not show the myelination ability *in vitro* (Figure 7A). Myelin sheath ultrastructure was detected after co-culture for 2 months and a compacted myelin structure was observed by transmission electron microscopy (Figure 7B).

To further confirm these results, we performed RNA sequencing to examine changes in the global expression profile of different developmental stages among hiPSCs, the NCSCs, and Schwann cells. The samples included undifferentiated hiPSCs and freshly isolated $P75^+/HNK1^+$ hiPSC NCSCs from control and CMT1A-1 groups, respectively, plus Schwann cell-differentiated NCSCs on day 28 from control, CMT1A-1, and PMP22 groups (GEO: GSE97851). The results demonstrated that the expression profile of undifferentiated hiPSCs in both control and CMT1A-1 group was enriched for genes related to pluripotency (*OCT4*, *SOX2*, *NANOG*, *REX1*, and others). However, the freshly isolated hiPSC NCSCs in the control and CMT1A-1 groups strongly expressed neural crest-specific transcription factors (e.g., *SOX10*, *SOX9*, *FOXD3*, *MSX1*, *MSX2*, *PAX3*, *PAX7*, and others) (Figure S6A). These results were in accordance with that of immunostaining assay of hiPSCs and NCSCs as described above. Meanwhile, *PMP22* was found to be expressed by NCSCs, and there was no statistical difference between CMT1A1 and control group as assayed by qRT-PCR (Figure S6B).

Nonetheless, Schwann cells differentiated from control NCSCs on day 28 were highly enriched in transcripts associated with SCP genes (*SOX10*, *AP2α*, *ERBB3*, *L1CAM*, and others), immature Schwann cell genes (*GFAP*, *S100B*, *OCT6*, and *NESTIN*), and markers of mature non-myelinating or myelinating Schwann cells (*MPZ*, *PLP1*, and others), while Schwann cells derived from CMT1A-1 and PMP22 groups had remarkably lower expression level of these genes. Moreover, other neural crest cells and/or Schwann cell relevant genes, including *TFAP2B*, *TFAP2C*, *HOXC4*, *OTX2*, and *ZIC3*, were expressed by control Schwann cells, while CMT1A-1 and PMP22 Schwann cells had far fewer transcripts of these genes. It was reported that *COL13A1* was expressed in neuromuscular junction and its defect would cause a decreased contact surface for neurotransmission because Schwann cells erroneously enwrapped nerve terminals and invaginated into the synaptic cleft (Latvanlehto et al., 2010). A lower expression level of *COL13A1* was found in CMT1A-1 and PMP22 Schwann cells when compared with that of control Schwann cells (Figures S6C and S6D). The exact role of these genes in CMT1A pathogenesis need to be further elucidated. Interestingly, the mRNA expression level of *PMP22* and numerous endoneurial fibroblast-like cell markers (*CD34*, *PDGFRB*, *FAP*, *FSP/S100A4*, and others) in the CMT1A-1 and PMP22 groups was noticeably higher in comparison with that of control cells (Figure S6E). qRT-PCR analysis further confirmed the results of mRNA sequencing (Figure S6F). These results

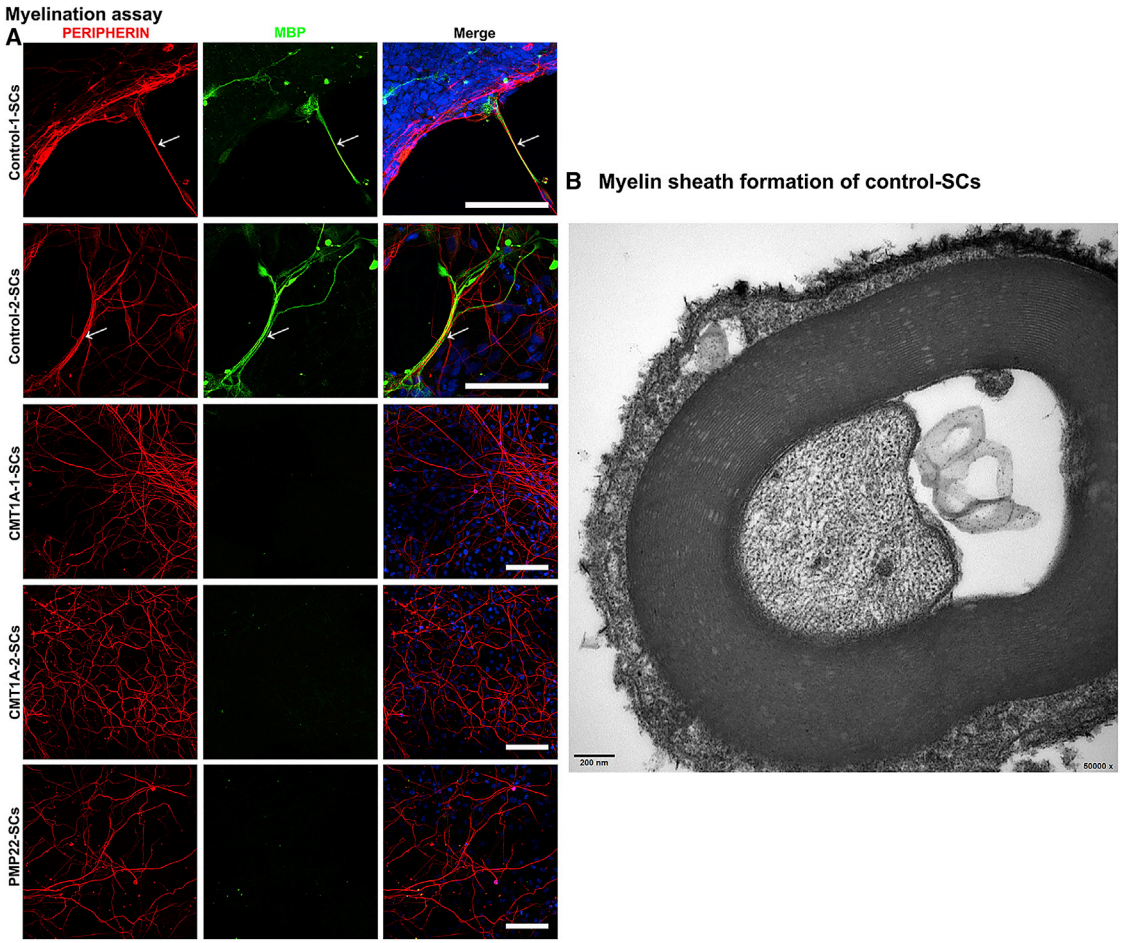

Figure 7. Control Schwann Cells Align and Myelinate Human iPSC-Derived Peripheral Neurons

(A) Myelinated segments were stained with anti-MBP and anti-PERIPHERIN in control group, while no myelination was detected in Schwann cells from the CMT1A and PMP groups (n = 5 independent experiments). The arrows indicate the myelinated cells. Scale bars, 100 μm.

(B) The myelin structure formed by control Schwann cells was viewed by electron microscopy (n = 4 independent experiments). Scale bar, 200 nm.

further indicated that PMP22 overexpression could result in a developmental switch in Schwann cell differentiation and promote the generation of EFLCs at the expense of Schwann cells.

Lipids including cholesterol are essential constituents of myelin (Saher et al., 2005). A previous study in a CMT1A mouse model indicated that the increased expression of PMP22 led to a strongly reduced expression of genes important for cholesterol synthesis and some other genes involved in lipid metabolism (Vigo et al., 2005). We thus analyzed the gene expression profile related to cholesterol synthesis and lipid metabolism and found that transcripts encoding HMG-coenzyme A (CoA) synthase (*HMGCS1*) and reductase (*HMGCR*), lysophospholipase (*LYPLA1*), and stearoyl-CoA desaturase (*SCD*) were substantially reduced in CMT1A-1 and PMP22 Schwann cells when compared with that of control Schwann cells. Surprisingly, we discovered that the expression level of apolipoprotein members including *APOA1*, *APOA2*, *APOB*, *APOC1*, and *APOC3* was greatly reduced in CMT1A-1 and PMP22 Schwann cells in comparison with the control group (Figure S6G). Moreover, most of these apolipoprotein members had been implicated in myelin biosynthesis and/or demyelination (Duan et al., 2007; Garcia-Mateo et al., 2014; Hunter et al., 2005; LeBlanc et al., 1989; Poliani et al., 2015; Zamel et al., 2008). Similar results were obtained when qRT-PCR detection of these samples was performed (Figure S6H).

The RNA sequencing data of Schwann cell-differentiated NCSCs from control and CMT1A groups was also analyzed using Ingenuity Pathways Analysis (IPA) software

(Table S1). We first investigated the overall gene list and analyzed these genes in terms of some important gene and cellular functions. The results indicated that important and statistically significant gene functions included fibrogenesis, autophagy, cell morphology, growth, migration, and cellular assembly/organization. Schwann cell-differentiated NCSCs from the CMT1A group showed significant upregulation of genes of fibrogenesis, formation of actin filaments and formation of actin stress fibers, which was consistent with our *in vitro* differentiation results as described above. Moreover, We also detected the upregulation of autophagy genes in CMT1A cells, while autophagy had been reported to be activated by PMP22 overexpression in a CMT1A mouse model (Fortun et al., 2006) and to play a central role in Schwann cell myelin breakdown (Gomez-Sanchez et al., 2015).

Canonical pathways were then identified and analyzed from the IPA libraries. The statistically significant canonical pathways included RhoGDI, PTEN, ERK/MAPK, mTOR, and EPHRIN receptor signaling pathways, among others. For example, RhoGDI and PTEN signaling pathways were reported to play important roles in proper myelination of the PNS (Cotter et al., 2010); nonetheless, downregulation of genes of these pathways were found in CMT1A cells when compared with the control group. We also detected upregulation of genes of ERK/MAPK, mTOR, and EPHRIN receptor signaling pathway in CMT1A cells. It was reported that hyperactivation of the Mek-Erk can be found in a CMT1A rat model (Fledrich et al., 2014) and rapamycin, an mTOR inhibitor, improved myelination in a PMP22 overexpression mice model (Rangaraju et al., 2010). Previous reports showed that Ephrin signaling regulates CNS myelination (Linneberg et al., 2015) and antibody-mediated neutralization of myelin-associated EphrinB3 accelerates CNS remyelination (Syed et al., 2016); however, whether Ephrin signaling plays a role in peripheral myelination remains to be elucidated.

DISCUSSION

Peripheral neuropathies are very common neurological disorders that can arise from different underlying causes, such as diabetes, infection, and heredity. CMT disease is the most common hereditary peripheral neuropathy involving dysfunction of the PNS, which comprises peripheral neurons and Schwann cells. CMT1A, which is the primary subgroup of CMT, is characterized by defects in the myelin-forming Schwann cells. Previous studies have used many types of transgenic CMT1A animal models to study Schwann cells and their functions in an effort to uncover the underlying pathogenesis of this disease (Sereda and Nave, 2006). However, most of these studies have usually focused on postnatal abnormities and have rarely considered the course of fetal development. Moreover, although rodent models have yielded important insights into some molecular mechanisms of disease development and/or facilitated the development of promising treatment strategies, they may not accurately recapitulate human disease because of basic differences in the anatomy, physiology, pathophysiology, and genetic background of human and mouse (Maries et al., 2003). For example, ascorbic acid was found to improve the locomotion and lifespan of CMT1A model mice through the remyelination of sciatic nerves (Passage et al., 2004), but a 2-year multi-center clinical trial revealed that ascorbic acid supplementation had no significant effect on neuropathy compared with placebo (Pareyson et al., 2011). Thus, a human-specific model will be of great value in uncovering the pathogenic mechanisms of CMT1A disease.

iPSCs offer an exciting approach through which we can generate patient-specific models and/or experimentally simulate the developmental process through directional differentiation. In the present study, we successfully established a CMT1A hiPSC model using hDFs from a single CMT1A patient and retroviral transduction of *OCT4*, *SOX2*, *c-MYC*, and *KLF4*. The CMT1A hiPSCs and control hiPSCs were generated with similar efficiencies. CMT1A hiPSCs retained the PMP22 duplication, exhibited a normal karyotype, expressed pluripotency markers (OCT4, NANOG, SOX2, SSEA4, and TRA-1-60), and could be differentiated into cell types of all three germ layers. These results show that *PMP22* duplication does not affect the reprogramming efficiency or pluripotency of hiPSCs. We thus next sought to simulate the process of PNS development by inducing CMT1A hiPSCs to differentiate into peripheral neurons and Schwann cells through NCSCs.

The PNS develops from NCSCs during the fetal development of vertebrates. Neural crest cells have been a focus of developmental biology research since they were first described in 1868, because they have strong migration/differentiation abilities and can generate diverse tissues (e.g., the PNS, glands, cartilage, bone, and teeth) (Crane and Trainor, 2006). When cultured *in vitro*, neural crest cells can give rise to a vast array of different cell types, such as MSCs, melanocytes, and nearly all the cells of the PNS, including autonomic neurons, sensory neurons, and supporting glial cells (i.e., Schwann cells) (Anderson, 2000). Previous studies indicated that dysfunction of the PNS may be an essential cause of CMT1A. Thus, neural crest cells represent an ideal model for studying the development of peripheral neurons and Schwann cells in CMT1A. In the present study, we induced CMT1A hiPSCs to differentiate into CMT1A NCSCs. We found that CMT1A NCSCs could be easily generated in a chemically defined system using an EB-formation strategy, and that

they could be purified by FACS with a high efficiency comparable with that seen in the control group. These results demonstrated that the overexpression of PMP22 did not affect the NCSC differentiation capacity of CMT1 hiPSCs.

We next subjected the generated CMT1A NCSCs to various *in vitro* assays. We found that the CMT1A and PMP22 NCSCs could be efficiently induced into MSCs and MSC derivatives, including osteogenic, adipogenic, chondrogenic, and smooth muscle lineages. Moreover, CMT1A and PMP22 NCSCs could be differentiated into peripheral neurons with the efficiency comparable with that of control cultures. Thus, the CMT1 NCSCs maintained their normal mesodermal and peripheral neuronal differentiation potential despite the increased gene dosage of PMP22.

When we cultured the cells under the conditions for Schwann cell differentiation, however, we found that CMT1A NCSCs rarely differentiated into typical Schwann cells (i.e., those co-expressing GFAP and S100B), but instead generated numerous fibroblast-like cells that expressed CD34. In this, the CMT1A NCSCs were significantly different from the normal control cells. Previous studies showed that the differentiation of an NCSC to a Schwann cell includes an intermediate stage called the Schwann cell precursor (SCP) (Jessen and Mirsky, 2005). SCPs have four major functions: to act as an intermediary precursor stage between NCSCs and Schwann cells (primary function); to provide essential trophic support for sensory and motor neurons; to provide important support for normal nerve fasciculation; and to act as the source for a small population of endoneurial fibroblasts (Jessen et al., 1994). The endoneurial fibroblasts, which often exist between nerve fibers in the endoneurium, express the cell surface marker, CD34 (Richard et al., 2012). Therefore, we believe that the aforementioned fibroblast-like cells represent endoneurial fibroblasts. We speculate that the generation of Schwann cells may be interrupted by the duplication of *PMP22* in CMT1A cells. Indeed, when we investigated whether an increased dosage of *PMP22* could affect the Schwann cell differentiation ability of normal hiPSCs, the PMP22-overexpressing hiPSCs recapitulated the Schwann cell differentiation defect of CMT1A NCSCs.

A previous report described the characteristic gene expression during Schwann cell lineage development. NCSCs (express *SOX10*, *AP2α*, *P75*, *ERBB3*, and others) can differentiate to SCPs (express *BFABP*, *DHH*, *P0*, *GAP43*, *PMP22*, *PLP1*, and others) and immature Schwann cells (express *GFAP*, *S100B*, *OCT6*, *O4*, and others) sequentially, the latter of which finally give rise to mature non-myelinating or myelinating Schwann cells (express the major myelin proteins *MBP* and *PLP1*, and the major structural protein in myelin, *MPZ*) (Jessen and Mirsky, 2005). We thus applied mRNA sequencing to detect the changes in gene expression profile during the Schwann cell differentiation of hiPSCs. Our results did not reveal significant differences in hiPSCs and NCSCs between CMT1A and control cells. However, the mRNA expression levels of SCP genes, immature Schwann cell genes, and markers of mature non-myelinating or myelinating Schwann cells were found to be substantially lower in the CMT1A-1 and PMP22 groups than in the control group, while transcripts of *PMP22* and endoneurial fibroblast-like cell markers were detected at higher levels in CMT1A-1 and PMP22 cells than that of control cells. These results further confirmed our observation of a developmental switch in PMP22-overexpression cells.

Demyelination or dysmyelination is considered to be the most common cause in the pathogenesis of CMT1A (Li et al., 2013). Here, our results indicated that only the control Schwann cells formed myelin when co-cultured with peripheral neurons *in vitro*, which also demonstrated that the aberrant *PMP22* gene copy numbers would greatly impair the myelination ability of Schwann cells. Fledrich et al. (2014) reported that soluble neuregulin-1 treatment promotes Schwann cell differentiation and myelination, preserves axons, and restores nerve function. Nevertheless, we did not observe similar effects of neuregulin-1 (20 ng/mL) during Schwann cell differentiation and myelination assay in CMT1A-1 and PMP22 groups. Overexpression of *PMP22* may also cause apoptosis in several cell types, including aging Schwann cells (Li et al., 2013). While in our study we found that differentiated cells in CMT1A-1, CMT1A-2, and PMP22 groups proliferated more quickly as shown by direct observation under microscopy and anti-Ki67 immunostaining, in contrast no obvious cell apoptosis was detected by TUNEL assay at different time points during Schwann cell differentiation process in all groups. These results indicated that the extra copy of *PMP22* may cause the changes of cell growth kinetics and the underlying mechanism remains largely unknown. Cholesterol biosynthesis and/or lipid metabolism were also found to be play important roles in myelin formation and CMT1A pathogenesis in an animal model (Li et al., 2013). We uncovered that some of the genes related to cholesterol synthesis and lipid metabolism including *HMGCS1*, *HMGCR*, *LYPLA1*, *SCD*, and apolipoproteins had considerably fewer transcripts in CMT1A-1 and PMP22 Schwann cells when compared with that of control Schwann cells. These results further demonstrated that the three copies of *PMP22* may cause dysregulation of cholesterol/lipid biosynthesis and transportation in CMT1A pathogenesis. Gene function and canonical pathways of Schwann cell-differentiated NCSCs from control and CMT1A groups were also analyzed by IPA software, whose results showed significant upregulation of genes of fibrogenesis and autophagy, downregulation of genes of RhoGDI and PTEN signaling pathways, and upregulation of genes of ERK/MAPK, mTOR, and EPHRIN receptor signaling in CMT1A cells compared with the control group. These results may

have important implications for uncovering the underlying mechanism of pathogenesis in CMT1A.

Conclusions

Based on our data, we inferred that *PMP22* duplication may lead to a developmental switch of Schwann cell differentiation toward EFLCs and may also cause excessive cell proliferation, defects in myelination ability, and dysregulation of cholesterol/lipid biosynthesis and transportation. Consequently, in addition to the demyelination/dysmyelination theory for CMT1A pathogenesis, developmental disabilities of Schwann cells should also be considered as an underlying cause of CMT1A pathogenesis (Figure S7). Our results may have important implications for uncovering the underlying mechanism and the development of a promising therapeutic strategy for CMT1A neuropathy.

EXPERIMENTAL PROCEDURES

Cell Culture

The patient-derived iPSC lines, including CMT1A-1 hiPSCs and CMT1A-2 hiPSCs, were propagated on Matrigel (BD Bioscience, San Diego, CA)-coated plates in E8 (Stem Cell Technologies) defined medium. Two hFF hiPSC lines (established in our laboratory; see Ke et al., 2013) were used as the control.

Additional Experimental Procedures

For more detailed and additional information, please see Supplemental Experimental Procedures.

ACCESSION NUMBER

The accession number for the RNA-seq data reported in this paper is GEO: GSE97851.

SUPPLEMENTAL INFORMATION

Supplemental Information includes Supplemental Experimental Procedures, seven figures, and five tables and can be found with this article online at https://doi.org/10.1016/j.stemcr.2017.11.013.

AUTHOR CONTRIBUTIONS

L.S., L.H., and R.H., collection and/or assembly of data, data analysis and interpretation, manuscript writing; W.H., H.W., X.L., Z.Z., J.S., and Q.K., collection and/or assembly of data; M.Z., X.L., Z.P., and H.S., provision of study material; A.P.X., W.L., and X.Y., conception and design, final approval of manuscript.

ACKNOWLEDGMENTS

This work was supported by the National Key Research and Development Program of China, Stem Cell and Translational Research (2017YFA0103403, 2017YFA0103802); the National Natural Science Foundation of China (81570487, 81425016, 81600400); the Natural Science Foundation of Guangdong Province (S2013030013305, 2016A030310250); the Southern China International Cooperation Base for Early Intervention and Functional Rehabilitation of Neurological Diseases (2015B050501003); Guangdong Provincial Engineering Center for Major Neurological Disease Treatment; Key Scientific and Technological Program of Guangzhou City (201704020223, 2014J4500031, 201510010024); Guangzhou Clinical Research and Translational Center for Major Neurological Diseases (201604020010); Frontier and Innovation of Key Technology Project in Science and Technology Department of Guangdong Province (2013B021800274, 2014B020225007, 2015B020228001, 2016B030229002, 2017B020231001); National Key Clinical Department and National Key Discipline of Neurology, Guangdong Provincial Key Laboratory for Diagnosis and Treatment of Major Neurological Diseases (2014B030301035); and The Fundamental Research Funds for the Central Universities (15ykcj156, 17ykzd07).

Received: May 16, 2017
Revised: November 16, 2017
Accepted: November 16, 2017
Published: December 21, 2017

REFERENCES

Anderson, D.J. (2000). Genes, lineages and the neural crest: a speculative review. Philos. Trans. R. Soc. Lond. B Biol. Sci. *355*, 953–964.

Berciano, J., Garcia, A., Calleja, J., and Combarros, O. (2000). Clinico-electrophysiological correlation of extensor digitorum brevis muscle atrophy in children with Charcot-Marie-Tooth disease 1A duplication. Neuromuscul. Disord. *10*, 419–424.

Cotter, L., Ozcelik, M., Jacob, C., Pereira, J.A., Locher, V., Baumann, R., Relvas, J.B., Suter, U., and Tricaud, N. (2010). Dlg1-PTEN interaction regulates myelin thickness to prevent damaging peripheral nerve overmyelination. Science *328*, 1415–1418.

Crane, J.F., and Trainor, P.A. (2006). Neural crest stem and progenitor cells. Annu. Rev. Cell Dev. Biol. *22*, 267–286.

Duan, R.S., Jin, T., Yang, X., Mix, E., Adem, A., and Zhu, J. (2007). Apolipoprotein E deficiency enhances the antigen-presenting capacity of Schwann cells. Glia *55*, 772–776.

Fledrich, R., Stassart, R.M., Klink, A., Rasch, L.M., Prukop, T., Haag, L., Czesnik, D., Kungl, T., Abdelaal, T.A., Keric, N., et al. (2014). Soluble neuregulin-1 modulates disease pathogenesis in rodent models of Charcot-Marie-Tooth disease 1A. Nat. Med. *20*, 1055–1061.

Fortun, J., Go, J.C., Li, J., Amici, S.A., Dunn, W.J., and Notterpek, L. (2006). Alterations in degradative pathways and protein aggregation in a neuropathy model based on PMP22 overexpression. Neurobiol. Dis. *22*, 153–164.

Garcia-Mateo, N., Ganfornina, M.D., Montero, O., Gijon, M.A., Murphy, R.C., and Sanchez, D. (2014). Schwann cell-derived Apolipoprotein D controls the dynamics of post-injury myelin recognition and degradation. Front. Cell. Neurosci. *8*, 374.

Gomez-Sanchez, J.A., Carty, L., Iruarrizaga-Lejarreta, M., Palomo-Irigoyen, M., Varela-Rey, M., Griffith, M., Hantke, J., Macias-Camara, N., Azkargorta, M., Aurrekoetxea, I., et al. (2015). Schwann cell autophagy, myelinophagy, initiates myelin clearance from injured nerves. J. Cell Biol. *210*, 153–168.

Hanemann, C.O., Gabreels-Festen, A.A., Stoll, G., and Muller, H.W. (1997). Schwann cell differentiation in Charcot-Marie-Tooth disease type 1A (CMT1A): normal number of myelinating Schwann cells in young CMT1A patients and neural cell adhesion molecule expression in onion bulbs. Acta Neuropathol. *94*, 310–315.

Hargus, G., Ehrlich, M., Hallmann, A.L., and Kuhlmann, T. (2014). Human stem cell models of neurodegeneration: a novel approach to study mechanisms of disease development. Acta Neuropathol. *127*, 151–173.

Hunter, M., Angelicheva, D., Tournev, I., Ingley, E., Chan, D.C., Watts, G.F., Kremensky, I., and Kalaydjieva, L. (2005). NDRG1 interacts with APO A-I and A-II and is a functional candidate for the HDL-C QTL on 8q24. Biochem. Biophys. Res. Commun. *332*, 982–992.

Jessen, K.R., Brennan, A., Morgan, L., Mirsky, R., Kent, A., Hashimoto, Y., and Gavrilovic, J. (1994). The Schwann cell precursor and its fate: a study of cell death and differentiation during gliogenesis in rat embryonic nerves. Neuron *12*, 509–527.

Jessen, K.R., and Mirsky, R. (2005). The origin and development of glial cells in peripheral nerves. Nat. Rev. Neurosci. *6*, 671–682.

Joseph, N.M., Mukouyama, Y.S., Mosher, J.T., Jaegle, M., Crone, S.A., Dormand, E.L., Lee, K.F., Meijer, D., Anderson, D.J., and Morrison, S.J. (2004). Neural crest stem cells undergo multilineage differentiation in developing peripheral nerves to generate endoneurial fibroblasts in addition to Schwann cells. Development *131*, 5599–5612.

Ke, Q., Li, L., Cai, B., Liu, C., Yang, Y., Gao, Y., Huang, W., Yuan, X., Wang, T., Zhang, Q., et al. (2013). Connexin 43 is involved in the generation of human-induced pluripotent stem cells. Hum. Mol. Genet. *22*, 2221–2233.

Latvanlehto, A., Fox, M.A., Sormunen, R., Tu, H., Oikarainen, T., Koski, A., Naumenko, N., Shakirzyanova, A., Kallio, M., Ilves, M., et al. (2010). Muscle-derived collagen XIII regulates maturation of the skeletal neuromuscular junction. J. Neurosci. *30*, 12230–12241.

LeBlanc, A.C., Foldvari, M., Spencer, D.F., Breckenridge, W.C., Fenwick, R.G., Williams, D.L., and Mezei, C. (1989). The apolipoprotein A-I gene is actively expressed in the rapidly myelinating avian peripheral nerve. J. Cell Biol. *109*, 1245–1256.

Lee, G., Chambers, S.M., Tomishima, M.J., and Studer, L. (2010). Derivation of neural crest cells from human pluripotent stem cells. Nat. Protoc. *5*, 688–701.

Lee, G., Kim, H., Elkabetz, Y., Al, S.G., Panagiotakos, G., Barberi, T., Tabar, V., and Studer, L. (2007). Isolation and directed differentiation of neural crest stem cells derived from human embryonic stem cells. Nat. Biotechnol. *25*, 1468–1475.

Li, J., Parker, B., Martyn, C., Natarajan, C., and Guo, J. (2013). The PMP22 gene and its related diseases. Mol. Neurobiol. *47*, 673–698.

Li, W., Huang, L., Lin, W., Ke, Q., Chen, R., Lai, X., Wang, X., Zhang, J., Jiang, M., Huang, W., et al. (2015). Engraftable neural crest stem cells derived from cynomolgus monkey embryonic stem cells. Biomaterials *39*, 75–84.

Linneberg, C., Harboe, M., and Laursen, L.S. (2015). Axo-glia interaction preceding CNS myelination is regulated by bidirectional Eph-Ephrin signaling. ASN Neuro *7*. https://doi.org/10.1177/1759091415602859.

Lupski, J.R., de Oca-Luna, R.M., Slaugenhaupt, S., Pentao, L., Guzzetta, V., Trask, B.J., Saucedo-Cardenas, O., Barker, D.F., Killian, J.M., Garcia, C.A., et al. (1991). DNA duplication associated with Charcot-Marie-Tooth disease type 1A. Cell *66*, 219–232.

Maries, E., Dass, B., Collier, T.J., Kordower, J.H., and Steece-Collier, K. (2003). The role of alpha-synuclein in Parkinson's disease: insights from animal models. Nat. Rev. Neurosci. *4*, 727–738.

Pareyson, D., Reilly, M.M., Schenone, A., Fabrizi, G.M., Cavallaro, T., Santoro, L., Vita, G., Quattrone, A., Padua, L., Gemignani, F., et al. (2011). Ascorbic acid in Charcot-Marie-Tooth disease type 1A (CMT-TRIAAL and CMT-TRAUK): a double-blind randomised trial. Lancet Neurol. *10*, 320–328.

Passage, E., Norreel, J.C., Noack-Fraissignes, P., Sanguedolce, V., Pizant, J., Thirion, X., Robaglia-Schlupp, A., Pellissier, J.F., and Fontes, M. (2004). Ascorbic acid treatment corrects the phenotype of a mouse model of Charcot-Marie-Tooth disease. Nat. Med. *10*, 396–401.

Poliani, P.L., Wang, Y., Fontana, E., Robinette, M.L., Yamanishi, Y., Gilfillan, S., and Colonna, M. (2015). TREM2 sustains microglial expansion during aging and response to demyelination. J. Clin. Invest. *125*, 2161–2170.

Rangaraju, S., Verrier, J.D., Madorsky, I., Nicks, J., Dunn, W.J., and Notterpek, L. (2010). Rapamycin activates autophagy and improves myelination in explant cultures from neuropathic mice. J. Neurosci. *30*, 11388–11397.

Richard, L., Topilko, P., Magy, L., Decouvelaere, A.V., Charnay, P., Funalot, B., and Vallat, J.M. (2012). Endoneurial fibroblast-like cells. J. Neuropathol. Exp. Neurol. *71*, 938–947.

Robaglia-Schlupp, A., Pizant, J., Norreel, J.C., Passage, E., Saberan-Djoneidi, D., Ansaldi, J.L., Vinay, L., Figarella-Branger, D., Levy, N., Clarac, F., et al. (2002). PMP22 overexpression causes dysmyelination in mice. Brain *125*, 2213–2221.

Saher, G., Brugger, B., Lappe-Siefke, C., Mobius, W., Tozawa, R., Wehr, M.C., Wieland, F., Ishibashi, S., and Nave, K.A. (2005). High cholesterol level is essential for myelin membrane growth. Nat. Neurosci. *8*, 468–475.

Sereda, M., Griffiths, I., Puhlhofer, A., Stewart, H., Rossner, M.J., Zimmerman, F., Magyar, J.P., Schneider, A., Hund, E., Meinck, H.M., et al. (1996). A transgenic rat model of Charcot-Marie-Tooth disease. Neuron *16*, 1049–1060.

Sereda, M.W., and Nave, K.A. (2006). Animal models of Charcot-Marie-Tooth disease type 1A. Neuromolecular. Med. *8*, 205–216.

Syed, Y.A., Zhao, C., Mahad, D., Mobius, W., Altmann, F., Foss, F., Gonzalez, G.A., Senturk, A., Acker-Palmer, A., Lubec, G., et al. (2016). Antibody-mediated neutralization of myelin-associated EphrinB3 accelerates CNS remyelination. Acta Neuropathol. *131*, 281–298.

Takahashi, K., and Yamanaka, S. (2006). Induction of pluripotent stem cells from mouse embryonic and adult fibroblast cultures by defined factors. Cell *126*, 663–676.

Vigo, T., Nobbio, L., Hummelen, P.V., Abbruzzese, M., Mancardi, G., Verpoorten, N., Verhoeven, K., Sereda, M.W., Nave, K.A., Timmerman, V., et al. (2005). Experimental Charcot-Marie-Tooth type 1A: a cDNA microarrays analysis. Mol. Cell. Neurosci. *28*, 703–714.

Zamel, R., Khan, R., Pollex, R.L., and Hegele, R.A. (2008). Abetalipoproteinemia: two case reports and literature review. Orphanet J. Rare Dis. *3*, 19.